J Solid State Electrochem (2007) 11:1023–1030
DOI 10.1007/s10008-007-0263-y

ORIGINAL PAPER

Preparation and spectroelectrochemical characterization of composite films of poly(3,4-ethylenedioxythiophene) with 4-(pyrrole-1-yl) benzoic acid

Barbara Kowalewska · Krzysztof Miecznikowski · Oktawian Makowski · Barbara Palys · Lidia Adamczyk · Pawel J. Kulesza

Received: 15 October 2006 / Revised: 28 October 2006 / Accepted: 3 November 2006 / Published online: 26 January 2007

Abstract The possibility of incorporation of 4-(pyrrole-1-yl) benzoic acid, PyBA, during electrodeposition of poly (3,4-ethylenedioxythiophene), PEDOT, is demonstrated here. The resulting novel composite material has been fabricated as moderately thin (ca 200–300 nm thick) PEDOT/PyBA film on electrode surface. As evidenced from scanning tunneling microscopy (STM) and scanning electron microscopy (SEM), morphology of the composite film is dense and granular, and it is composed of larger granules in comparison to the PyBA-free PEDOT film. It is apparent from infrared reflectance absorption spectroscopy and spectroelectrochemical measurements that the PEDOT/PyBA composite film cannot be viewed as simple mixtures of PEDOT and PyBA components. Some specific (chemical) interactions between PEDOT and PyBA can be expected. The conducting polymer serves as a robust, positively charged conductive polmer matrix for anionic (carboxylate-group derivatized) partially polymerized PyBA structures. Upon incorporation of PyBA, the overall stability of PEDOT film (resistance to dissolution during prolonged voltammetric potential cycling) has been improved. The fact, that the composite PEDOT/PyBA film is capable of preconcentrating (under open circuit conditions) both cations (Cu^{2+}) or anions $\left(Fe(CN)_6^{3-}\right)$, implies the presence of both free (available for binding) carboxylate groups and positively charged PEDOT sites. The presence of PyBA in PEDOT seems to facilitate charge propagation in the composite film.

Keywords Poly(3,4-ethylenedioxythiophene)/PEDOT · 4-(pyrrole-1-yl) benzoic acid · Composite films · Electrodeposition · Microscopic examination · Spectroelectrochemistry

Introduction

During recent years, films based on organic conducting polymers have drawn considerable attention due to their potential utility in such different technologies as displays and light emitting diodes, smart windows, sensors, catalysis, secondary batteries and redox capacitors [1–4]. In the latter case, conducting polymers and related systems are promising materials for delivering high energy and power density. Among the polymers, PEDOT or poly(3,4-ethylenedioxythiophene) and its derivatives have been recognized as one of the most stable systems currently available [5–15]. For example, PEDOT has been used to fabricate antistatic coatings [16], conductive electrodes in light emitting diodes [17], and as a material for electrochromic devices [18, 19]. PEDOT films are known to be very stable in their oxidized (doped) states [7, 9–11] where they have even been reported to reach conductivity as high as 200 S cm^{-1} [20]. Somewhat lower conductivities have also been

"Contribution to the International Workshop on Electrochemistry of Electroactive Materials (WEEM-2006), Repino, Russia, 24–29 June 2006".

B. Kowalewska · K. Miecznikowski · O. Makowski · B. Palys · P. J. Kulesza (✉)
Department of Chemistry, University of Warsaw,
Pasteura 1,
02-093 Warsaw, Poland
e-mail: pkulesza@chem.uw.edu.pl

L. Adamczyk
Division of Chemistry, Department of Materials Engineering and Applied Physics, Technical University of Czestochowa,
Armii Krajowej 19,
42-200 Czestochowa, Poland

reported [21]. The conductivity of PEDOT films [22] obviously reflects the polymer morphology, the method of its fabrication, measurement, and experimental conditions. Although exact nature of the electrochemical responses of PEDOT films [23] is not well understood, it is generally believed that the system redox behavior originates from multiple overlapping redox transitions that are characterized by fast dynamics of charge propagation [24]. PEDOT has been successfully used as a robust conductive matrix for immobilization of metals, functionalized dopants, and redox and reactive centers [25–29].

Formation of PEDOT films was achieved chemically or electrochemically, and the overall polymerization involved oxidation of the 3,4-ethylenedioxythiophene (EDOT) monomer typically performed in organic nonaqueous solvents rather than in aqueous solutions. Because of the low solubility of thiophene monomers in water, electrodeposition of PEDOT in aqueous electrolytes was not common. Nevertheless, the possibility of use of aqueous anionic micellar media containing dodecyl sulfates for the fabrication of PEDOT films on electrode surfaces was demonstrated [30, 31]. The presence of anionic micelle was found to improve structural properties of the resulting PEDOT films. The colloidal aqueous solutions of PEDOT (that could be used to deposit the polymer films) were obtained by chemical oxidation (using potassium peroxysulfate) of EDOT monomer in the presence of polystyrenesulfonic acid [32]. The fact that aqueous solutions of phosphoric acid [33] and heteropoly acids [34] had been historically found to facilitate electropolymerization of thiophenes was later explored to produce (from aqueous solutions) well-behaved hybrid (composite) films of PEDOT with polyoxometallate (phosphomolybdate and phosphotungstate) redox centers [35]. Polyoxometallate templates combined with the layer-by-layer approach were also applied to produce multilayered systems containing ultrathin films of PEDOT interlayers with and without carbon nanoparticles or nanotubes [36–38]. Electrodeposition of PEDOT was successfully achieved in the presence of polynuclear metal hexacyanoferrates including Prussian blue [39, 40]. It can be rationalized that the concept of combining PEDOT with largely hydrophilic polynuclear anionic species shows promise for designing new composite materials of functionality.

In the present work, we propose a novel composite material consisting of PEDOT and partially polymerized 4-(pyrrole-1-yl) benzoic acid (PyBA). The latter carboxylate-derivatized organic component was previously demonstrated to form (with Prussian blue) crack-free composite materials of utility to the construction of optical [41] and amperometric sensors [42]. We also refer here to the recent concepts of fabrication (electrodeposition) of three-dimensional composite (hybrid) films in which anionic organic or inorganic species are attracted and electrostatically stabilized by positively charged conducting polymer backbone [36–38, 43–46]. Our ultimate goal has been to produce robust PEDOT-based films of high charge propagation dynamics in which, by introduction of the negatively charged (carboxylate containing) PyBA matrix, the overall stability will be improved. We address the physicochemical identity of our composite film using electrochemical, spectroscopic, and microscopic techniques.

Experimental

All chemicals were of analytical grade purity, and they were used as received. In particular, PyBA and EDOT monomer were obtained from Aldrich. Solutions were prepared using doubly distilled subsequently deionized (Millipore Milli-Q) water. Experiments were carried out at room temperature.

Electrochemical measurements were done with CH Instruments (Model CHI 660B) workstation (Austin, U.S.A.). A standard three-electrode cell with magnetic stirrer was used for the electrochemical preparation and characterization of composite films. The working electrode was glassy carbon of 3 mm diameter supplied by Bioanalytical Systems (BAS), (West Lafayette, IN, U.S.A.). Before modification, a glassy carbon electrode was activated by polishing with fine grade aqueous alumina slurries (grain size, 5–0.5 μm) on a polishing piece of cloth. The counter electrode was made from Pt wire. All potentials were expressed vs the saturated (KCl) Ag/AgCl electrode. Gold-covered foil (geometric area, 1.5 cm^2) was used as an optically transparent working electrode for spectrochemical investigations of PEDOT-based films.

Gold-covered foil electrode substrates were prepared by evaporation of gold onto transparency foil (for copiers, PP2500 from 3 M) using Balzers Unin MED 010 sputtering system. Before evaporation, the foil was soaked in ethyl alcohol and subjected to ultrasonic cleaning for 2 h. The thickness of gold was ca 25 nm. A Hewlett-Packard 8452A diode array spectrophotometer was used together with the electrochemical analyzer to obtain spectroelectrochemical data and voltabsorptometric responses in the visible range. The spectra were recorded at 1 s intervals corresponding to 5 mV steps or 5 mV s^{-1} scan rate. The spectroelectrochemical cell was manufactured from 2.5 mm thick quartz cuvette. The gold-covered foil was inserted into the optical path. The upper, broader path of the cell accommodated a KCl-saturated Ag/AgCl reference electrode and Pt counter electrode.

The composite layers of PEDOT with PyBA were grown on glassy carbon and Au-covered foil electrode substrates by potential cycling (at 50 mV s^{-1}) in the 0.2 mol dm^{-3} H_2SO_4 solutions for modification containing EDOT and

PyBA at the saturation levels. Typically, 25 full potential cycles, starting from −0.400 and ending at 1.100 V, were applied.

Scanning electron microscopy (SEM) images were obtained using LEO 435 VP (Germany). The microscope was equipped with EDX analyzer. Scanning tunneling microscopy (STM) images were obtained ex situ (in air) using EasyScan Nanosurf (Switzerland) instrument. The tips of Pt/Ir (90/10) wires of 0.25 mm diameter were formed mechanically, and they were used as probes. The scanning step was achieved in the constant-current mode at the positive sample bias of 50–100 mV and tunneling current of 1–2 nA. Infrared spectra were measured with Shimadzu 8400 Fourier transform infrared (FTIR) spectrometer. The infrared reflectance absorption spectra (IRRAS) were recorded using a Specular Reflectance Accessory Model 500 produced by Spectra Tech. The beam incidence angle was equal to 80° with respect to the surface normal. Typically, 500 scans were averaged for single reflectance spectrum.

Results and discussion

Fabrication and voltametric characterization of PyBA/PEDOT film

Electrodeposition of composite films of poly(3,4-ethylenedioxythiophene), with 4-(pyrrole-1-yl) benzoic acid (PEDOT/PyBA) was achieved by voltammetric potential cycling in the mixture for modification as described in the Experimental section. General features of the fabrication of PEDOT-based films in acid media had been described earlier [35]. The growth of both PEDOT (Fig. 1a) and PEDOT/PyBA (Fig. 1b) films was evident from the increase of voltammetric currents. The composite film tended to grow somewhat faster. It is reasonable to expect that PEDOT structures were generated on the electrode surface during positive potential scans [3, 7–24, 35, 36]. During formation of the PEDOT/PyBA composite film, the positively charged PEDOT structures were likely to interact electrostatically with the anionic carboxylate groups of PyBA. The latter characteristics should lead to the increased stability of the PEDOT/PyBA composite film. In both cases (Fig. 1a and b), the most pronounced film growth occurred during the first voltammetric cycles in the solution for modification. It was also apparent from the parallel experiments performed in the PyBA-containing (but EDOT-free) solution that under the potential cycling conditions of Fig. 1, no appreciable deposition of PyBA (relative to the PEDOT-based systems) on the electrode surface occurred.

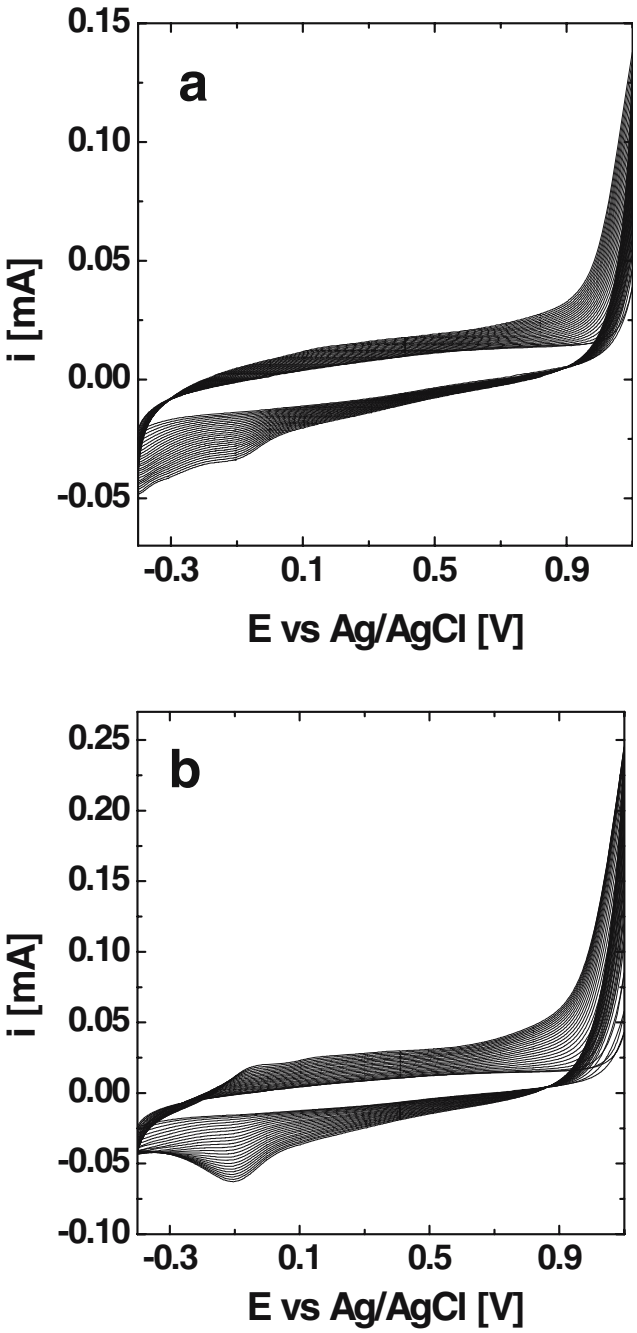

Fig. 1 Cyclic voltammograms illustrating electrodeposition of **a** PEDOT and **b** PyBA/PEDOT films on glassy carbon from the solutions for modification. Scan rate, 50 mV/s. Electrode geometric area, 0.071 cm^2

The choice of experimental parameters (scan rate or potential limits) had some effect on the formation of PEDOT/PyBA films. An increase of the upper potential limit (during voltammetric cycling) toward a more positive value (e.g., to 1.3 V) led to the faster film growth but resulted in its poorer adherence. Application of a faster scan rate (e.g., 500 mV s^{-1}) required much longer cycling times

to produce a film of the comparable loading to that of Fig. 1b. The electrodeposition parameters chosen here seemed to be optimum in terms of reproducibility and the overall system's stability.

Figure 2 illustrates cyclic voltammograms of (a) PEDOT and (b) PEDOT/PyBA films recorded in 0.2 mol dm^{-3} H_2SO_4 after their electrodeposition (performed in a manner as in Fig. 1a and b). Although both responses were similar in nature, the voltammetric currents of the PEDOT/PyBA composite film were higher in comparison to those of PEDOT. This observation could originate from the relatively larger loading of the composite film on the electrode surface and/or from the faster dynamics of charge (electrons, counterions) propagation during voltammetric potential cycling. Profilometric experiments (done using Talysurf 50, Rank Taylor Hobson) showed that both films had comparable thicknesses, ca 200 nm.

We also found that both Cu^{2+} and $Fe(CN)_6^{3-}$ ions can be preconcentrated into the composite PEDOT/PyBA films by exposing them (independently) to 5 mmol dm^{-3} solutions of $CuSO_4$ and $K_3[Fe(CN)_6]$, respectively, for 30 min under open circuit conditions. To verify the presence of Cu^{2+} and $Fe(CN)_6^{3-}$ within the film, the ions were reduced (to Cu^0 and $Fe(CN)_6^{4-}$) by recording linear scan voltammograms in 0.5 mol dm^{-3} H_2SO_4 (see dotted and solid lines in inset of Fig. 2). The result was consistent with the view that both carboxylate groups (from PyBA) and positively charged PEDOT sites were available in the PEDOT/PyBA composite film, and they were free to bind Cu^{2+} and $Fe(CN)_6^{3-}$ ions. The fact that the $Fe(CN)_6^{3-/4-}$ reduction (one-electron) voltammetric peak was significantly larger than that for the $Cu^{2+/0}$ reduction (two-electron) implied that the composite film contained a larger population of positively charged PEDOT relative to carboxylate-containing PyBA sites.

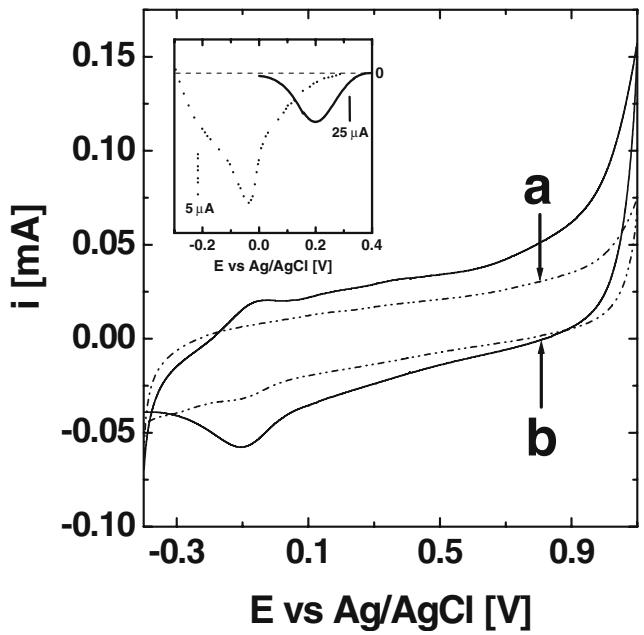

Fig. 2 Comparison of cyclic voltammetric responses of **a** PEDOT and **b** composite PyBA/PEDOT films. Scan rate, 50 mV s^{-1}. Electrolyte: 0.2 mol dm^{-3} H_2SO_4. *Inset* shows linear scan voltammetric reduction peaks for the reductions of Cu^{2+} (*dotted line*) and $Fe(CN)_6^{3-}$ (*solid line*) ions that have been preconcentrated in the composite film under open circuit conditions

The stability of the composite PEDOT/PyBA film was diagnosed by subjecting the system to the long-term voltammetric potential cycling in 0.2 mol dm^{-3} H_2SO_4 electrolyte within the selected potential limits. For example, in the following potential cycling for 4 h within the potential range −0.2 to 0.8 V, the overall decrease of voltammetric currents did not exceed 5%. It is reasonable to expect that this current decrease originates from the surface dissolution of composite film (in contact with liquid supporting electrolyte) rather than structural degradation of the material. On the whole, the result is consistent with good stability of the composite system. The most likely explanation of the stabilization effect takes into account the existence of electrostatic attraction forces between positively charged PEDOT polymer (in conducting state) and the existence of carboxylate groups in PyBA that could be anionic. When the analogous experiment was performed using simple PEDOT film, the current decrease was observed on the level close to 8–9%.

Dynamics of charge transport

Cyclic voltammetric currents of Fig. 2 have been found proportional to scan rate up to at least 200 mV s^{-1}. Thus, despite the fact that thickness of our PEDOT-based films exceeds a monolayer-type coverage, the system exhibits surface-type behavior characteristic of the thin-layer limit [47, 48]. Certainly, the overall charge propagation must have been fast. At higher scan rates (>500 mV s^{-1}), the voltammetric currents have started to be proportional to the square root of scan rate. Such conditions are equivalent to the application of relatively short experimental times where the diffusion layer thickness is smaller than the film thickness. The latter behavior is consistent with the semi-infinite linear diffusion limit.

To get better insight into the dynamics of charge transport, we have recorded dependencies (Fig. 3) of the chronocoulometric charge (Q) on the square root of time ($t^{1/2}$). Such plots have diagnostic meaning [47, 48] because it is easy to distinguish between the semi-infinite linear diffusion charge propagation mechanism and the thin-layer-like behavior. It comes from the shape of the plots of Fig. 3 that two distinct patterns related to two time domains exist. For longer experimental (potential step) times applied, the thin-layer limit becomes operative, and the dependence of Q on $t^{1/2}$ flattens (Fig. 3) as a result of almost complete

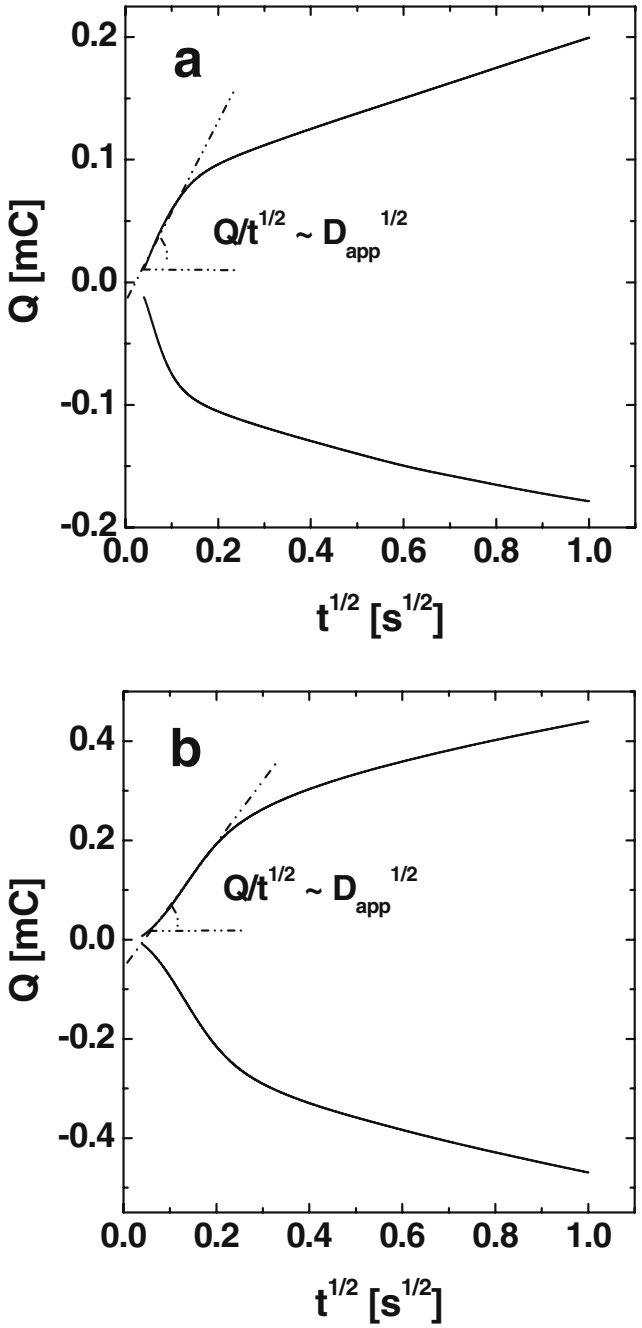

Fig. 3 Double potential step chronoculometric plots for **a** PEDOT and **b** PEDOT/PyBA films deposited on glassy carbon. A forward potential step was from 1.1 to −0.4 V. Electrolyte: 0.2 mol dm^{-3} H_2SO_4

electrolysis (reduction or oxidation) of the film. This situation is equivalent to the surface type behavior of the film under cyclic voltammetric conditions at lower scan rates (up to 200 mV s^{-1}), where currents have been proportional to scan rate. Judging from the appearance of linear portions in the chronocoulometric plots (Fig. 3) at shorter time scales, existence of the diffusional type patterns can be postulated here too. Under such conditions, the semi-infinite linear diffusion limit, where the diffusion layer thickness ($[2D_{app}t]^{1/2}$) is much smaller than the film thickness (d), applies. Thus, the dependence of Q on $t^{1/2}$ can be described in terms of the integrated Cottrell equation:

$$\left[Q/t^{1/2}\right] = 2nF\pi^{1/2}r^2\left[D_{app}^{1/2}C_o\right] \quad (1)$$

where r, D_{app}, C_o stand for the radius, apparent diffusion coefficient for charge propagation, concentration of redox centers, respectively, and other parameters either have been discussed above or have their usual significance. From the linear portion of the dependence of Q on $t^{1/2}$, one can determine the slope, $[Q/t^{1/2}]$, and indirectly, the kinetic parameter, $[D_{app}{}^{1/2}C_o]$. It should be remembered that the Q–$t^{1/2}$ chronocoulometric plot also permits to comment on possible ohmic and kinetic limitation effects that appear as a positive deviation from linearity and produce a sizeable negative intercept, respectively [48]. Judging from the data of Fig. 3, the above limitations have been rather small, and therefore, they have been neglected.

Figure 3 illustrates typical chronocoulometric responses recorded for the (a) PEDOT and (b) PEDOT/PyBA films. For comparative purposes, we consider here the reduction potential steps from 1.1 to −0.4 V. The linear portion of the plot in Fig. 3b is characterized by a higher slope (1.25 mC $s^{-1/2}$) relative to that of Fig. 3a (0.80 mC $s^{-1/2}$). In other words, the $[Q/t^{1/2}]$ value of Fig. 3b is ca 1.6 times higher than that of Fig. 3a. This result implies that the PEDOT/PyBA film may be characterized by the larger $[D_{app}{}^{1/2}C_o]$ kinetic parameter. The increase of $[D_{app}{}^{1/2}C_o]$ is likely to originate from the fact that the PEDOT/PyBA film contains carboxylate groups; thus, it is more hydrophilic and more open to the flux of ions. In the above discussion, the value of C_o is unknown, but it is not expected to be drastically different in the cases of PEDOT and PEDOT/PyBA films. Thus, it is reasonable to expect that the $Q/t^{1/2}$ slope becomes here a measure of the transport coefficient, D_{app}.

Microscopic and spectrochemical properties

Using STM (Fig. 4) and SEM (Fig. 5), we have examined and compared morphologies of (a) the single component, PEDOT, and (b) the composite, PEDOT/PyBA, films (deposited on glassy carbon). STM measurements permit to characterize systems on the nanometer level. While the structures are granular in both cases, the actual sizes and distribution of grains are different for PEDOT in comparison to those of PEDOT/PyBA. The size of PEDOT granules (Fig. 4a) seems to be smaller (20–30 nm) relative to the PEDOT/PyBA granules (Fig. 4b) reaching, or even exceeding, 100 nm. It is difficult to explain the difference in terms of the ability of PyBA to occupy the space between

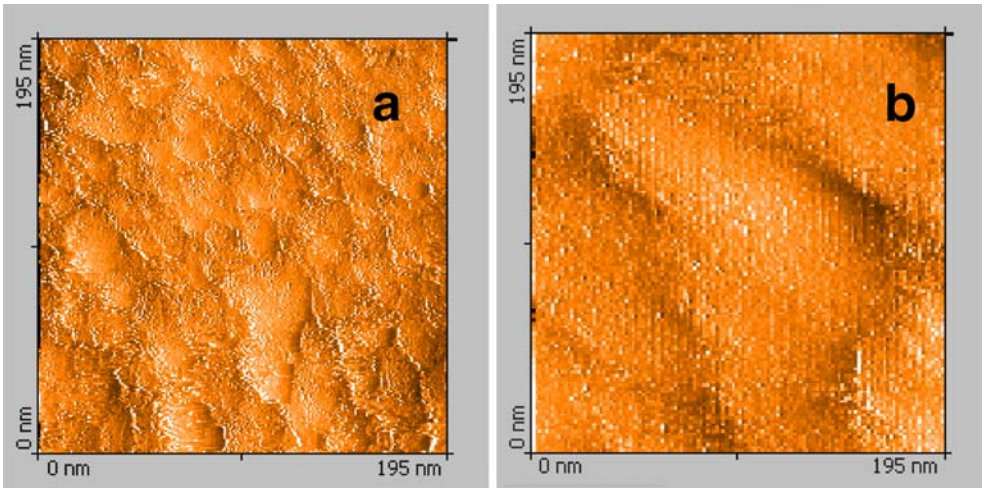

Fig. 4 STM images of **a** PEDOT and **b** composite PEDOT/PyBA films of glassy carbon (prepared as for Fig. 1a and b)

PEDOT granules. More likely, the carboxylate-containing PyBA units link the positively charged PEDOT nanostructures to form larger sub-microstructures. When the morphology of both films have been examined on the micrometer scale using SEM, the tendency to form larger agglomerates has been much more pronounced for the PEDOT/PyBA film (Fig. 5b) rather than PEDOT film (Fig. 5a).

To get better insight into nature of interactions of PyBA with PEDOT within the composite film, we performed ex situ FTIR measurements (by reflectance) of the glassy carbon electrode surfaces modified with (a) PEDOT and (b) PEDOT/PyBA. Comparison was also made with the reflectance spectrum of PyBA (deposited on glassy carbon (Fig. 6c). In the latter case, the PyBA film was fabricated in manner analogous to that of the composite film, except that only PyBA component was present in the mixture for modification. Contrary to PEDOT [35], or polyaniline [3, 44], during voltammetric potential cycling of PyBA, no sizeable currents or peaks were observed. Indeed, PyBA formed much thinner and practically nonelectroactive films on the electrode surface. It was also apparent upon comparison of infrared spectra of PyBA in KBr (for brevity not shown here) with those characteristic of PyBA deposited as utrathin film on glassy carbon (Fig. 6c) that PyBA underwent some polymerization (around the pyrrole ring) after voltammetric potential cycling. More detailed discussion will be a subject of our separate publication.

The spectrum of PEDOT/PyBA film (Fig. 6b) cannot be considered as a simple superposition of the PEDOT (Fig. 6a) and PyBA (Fig. 6c) spectra. For example, the characteristic bands of PEDOT are not only shifted but significantly altered upon incorporation of PyBA. Also new bands (e.g., at 640 cm^{-1}) are visible in the PEDOT/PyBA spectrum. On the other hand, the characteristic band of PyBA at 2,137 cm^{-1} disappears upon formation of the composite film. Furthermore, the PEDOT and PEDOT/PyBA samples seem to differ in the oxidation state. Indeed, the latter spectrum contains so-called doping-induced bands in the range 900–1,300 cm^{-1} [10]. Thus, more specific (than simple electrostatic) chemical interactions between PyBA and PEDOT can be expected within the composite film.

We also considered visible spectra of (a) PEDOT and (b) PEDOT/PyBA films (deposited on Au-covered foil) upon application of negative, −0.3 V (Fig. 7), and positive, 0.7 V (Fig. 8), potentials. Inset C illustrates the spectrum of the PyBA film deposited on Au-covered foil; it has been found

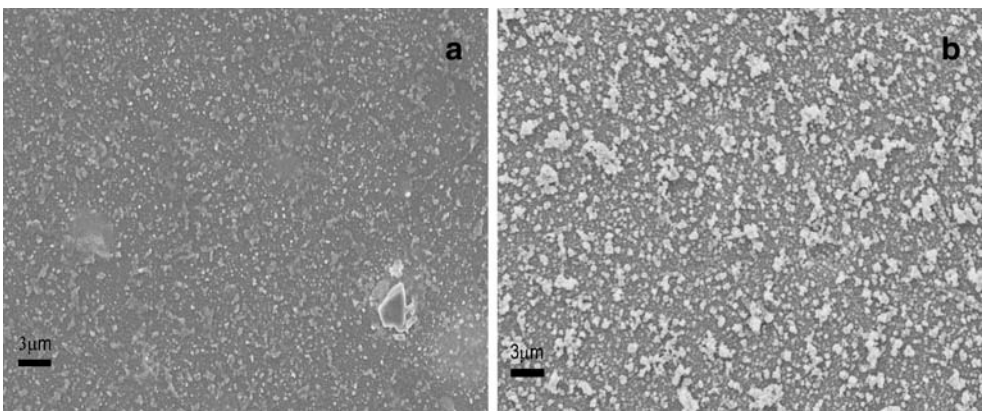

Fig. 5 SEM examination of glassy carbon surfaces modified with **a** PEDOT and **b** composite PEDOT/PyBA films. The films were grown as in Fig. 1

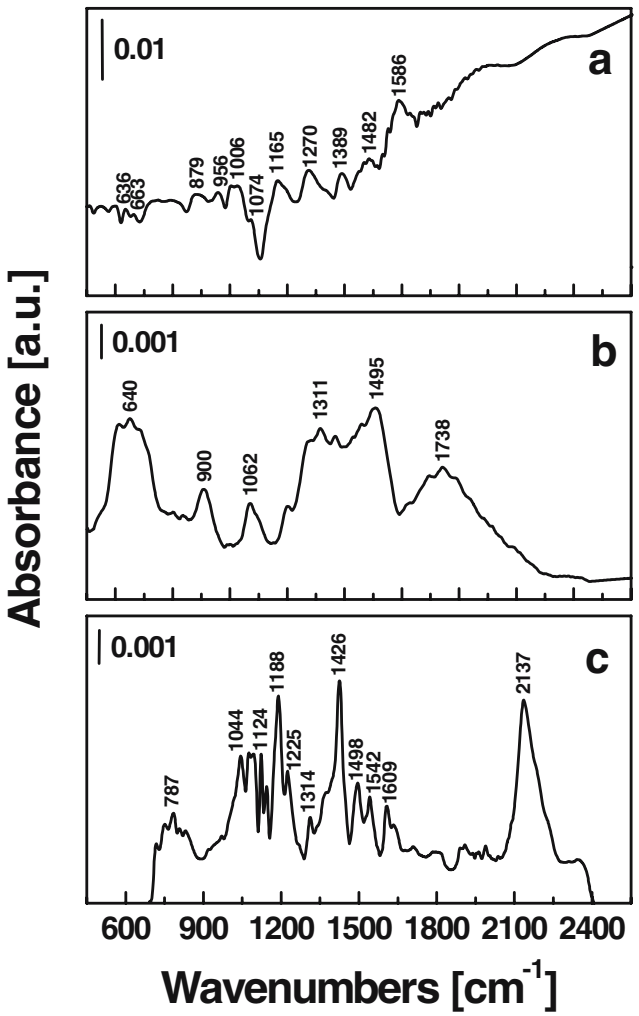

Fig. 6 FTIR spectra of **a** PEDOT, **b** PEDOT/PyBA, and **c** PyBA films deposited on glassy carbon

to be practically independent of the applied potential. In the case of both oxidized and reduced films, the respective spectra of PEDOT and PEDOT/PyBA were similar but not identical. The differences involved some shifts (on the level 30–50 nm) in the absorption maxima or minima.

Conclusions

The results are consistent with the view that the PEDOT/PyBA composite film is not only characterized by good physicochemical stability (understood in terms of resistance to degradation during repetitive potential cycling) and compact (dense) morphology, but it is also capable of effective propagation of charge (that could be useful in mediation of various redox reactions). Regardless the nature of interactions between PEDOT and PyBA components, the composite PEDOT/PyBA system cannot be considered as a simple mixture of these components. As

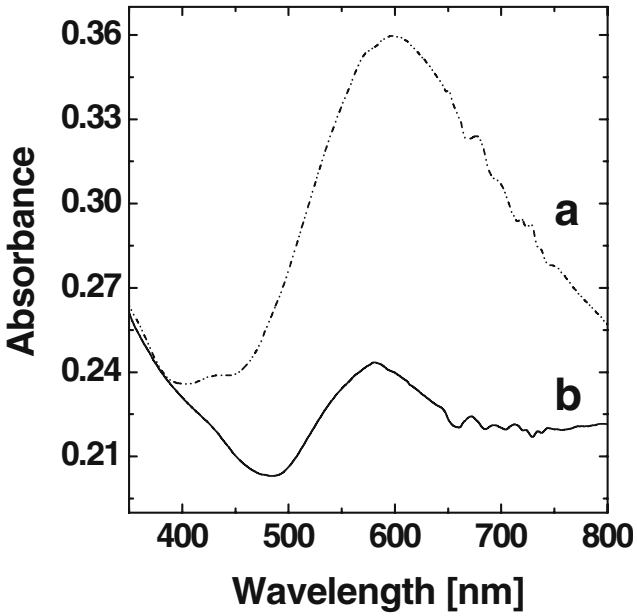

Fig. 7 Visible spectra of **a** PEDOT and **b** PEDOT/PyBA films (deposited on gold-covered foil) recorded upon application of −0.3 V. Electrolyte: 0.2 mol dm^{-3} H_2SO_4

the material contains functional (carboxylate) groups, it is reasonable to expect that by analogy to the previous work [42], it can be further modified via immobilization of enzyme molecules. The possibility of controlled preconcentration of certain metal cations and inorganic anions permits fabrication of novel hybrid conducting polymer-based materials [49]. The research is of importance to the

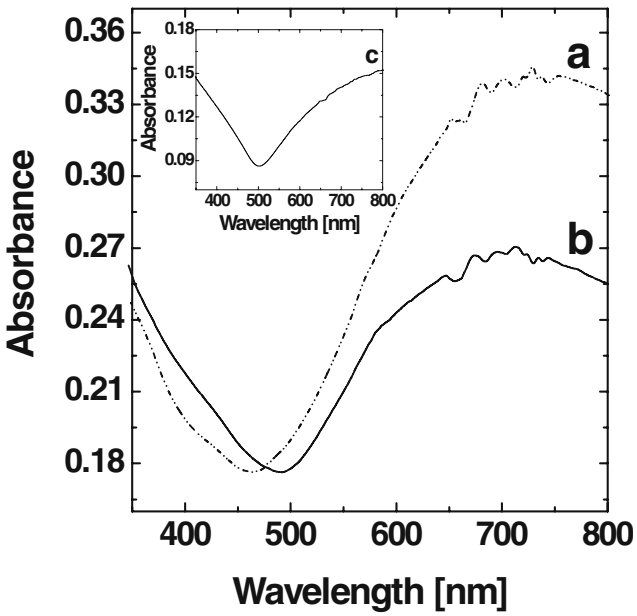

Fig. 8 Visible spectra of **a** PEDOT and **b** PEDOT/PyBA films (deposited on gold-covered foil) recorded upon application of 0.7 V. Electrolyte: 0.2 mol dm^{-3} H_2SO_4. *Inset* (**c**) shows spectrum of PyBA film. Electrolyte: 0.2 mol dm^{-3} H_2SO_4

development of nanostructured and functionalized PEDOT-based hybrid materials of potential utility in catalysis or electrocatalysis and to the construction of analytical sensors, biosensors, protective films, and charge-storage devices.

Acknowledgement This work was supported by Ministry of Science and Higher Education under the KBN Projects 7 T09A 05426 and 3 T09A 04427 (doctoral). A gift of EDOT monomer from Bayer is highly appreciated.

References

1. Nalwa HS (ed) (1997) Handbook of conductive molecules and polymers, vols 1–4, Wiley, New York
2. Barsukov V, Chivikov S, Barsukov I, Motronyuk T (1996) In: Barsukov V, Beck F (eds) New promising electrochemical systems for rechargeable batteries. Kluwer, Dordrecht, p 419
3. Inzelt G, Pineri M, Schultze JW, Vorotyntsev MA (2000) Electrochim Acta 45:2403
4. Rubinson JF, Mark HB (1999) In: Wieckowski A (ed) Interfacial electrochemistry, Ch 37, conducting polymer films as electrodes. Marcel Dekker, New York
5. Inzelt G (1994) In: Bard AJ (ed) Electroanalytical chemistry, vol 18. Marcel Dekker, New York
6. Jonas F, Schrader L (1991) Synth Met 41:831
7. Dietrich M, Heinze J, Heywang G, Jonas F (1994) J Electroanal Chem 369:87
8. Granstrom M, Berggren M, Inganas O (1995) Science 267:1479
9. Mastragostino M, Arbizzani C, Bongini A, Barbarella G, Zambianchi M (1992) Electrochim Acta 38:135
10. Kvarnstrom C, Neugebauer H, Blomquist S, Ahonen HJ, Kankare J, Ivaska A (1999) Electrochim Acta 44:2739
11. Lacroix JC, Kanazawa KK, Diaz AD (1989) J Electrochem Soc 136:1308
12. Heywang G, Jonas F (1992) Adv Mater 4:116
13. Gustafsson JC, Liedberg B, Inganas O (1994) Solid State Ion 69:145
14. Panero S, Passerini S, Scrosati B (1993) Mol Cryst Liq Cryst 229:97
15. Lampert CM (1984) Sol Energy Mater 11:1
16. Jonas F, Heywang G (1994) Electrochim Acta 39:1345
17. Gustafsson JC, Inganas O (1995) Adv Mater 7:1012
18. Sapp SA, Sotzing GA, Reddinger JL, Reynolds JR (1996) Adv Mater 8:808
19. Lin TH, Ho KC (2006) Sol Energy Mater 90:506
20. Pei Q, Zuccarello G, Heinze J, Heywang G, Jonas F (1994) J Electroanal Chem 369:87
21. Morvant MC, Reynolds JR (1998) Synth Met 92:57
22. Sundfords F, Bobacka J, Ivaska A, Lewenstam A (2002) Electrochim Acta 47:2245
23. Chen X, Inganas O (1996) J Phys Chem 100:15202
24. Bobacka J, Lewenstam A, Ivaska A (2000) J Electroanal Chem 489:17
25. Lisowska-Oleksiak A, Kazubowska K, Kupniewska A (2001) J Electroanal Chem 501:54
26. Noel V, Randriamahazaka H, Chevrot C (2000) J Electroanal Chem 489:46
27. Arbizzani C, Mastragostino M, Rossi M (2002) Electrochem Commun 4:545
28. Krishnamoorthy K, Kanungo M, Ambade AV, Contractor AQ, Kumar A (2002) Synth Met 125:441
29. Shan J, Pickup PG (2000) Electrochim Acta 46:119
30. Sakmeche N, Aaron JJ, Aeiyach S, Lacaze PC (2000) Electrochim Acta 45:1921
31. Sakmeche N, Aaron JJ, Fall M, Aeiyach S, Jouni M, Lacroix JC, Lacaze PC (1996) J Chem Soc Chem Comm 2727
32. Jonas F, Kraft W, Muys B (1995) Macromol Symp 100:169
33. Dong S, Zhang W (1998) Synth Met 30:359
34. Bidan G, Genies GM, Lapkowski M (1989) Synth Met 31:327
35. Adamczyk L, Kulesza PJ, Miecznikowski K, Palys B, Chojak M, Krawczyk D (2005) J Electrochem Soc 152:E98
36. Karnicka K, Chojak M, Miecznikowski K, Skunik M, Baranowska B, Kolary A, Piranska A, Palys B, Adamczyk L, Kulesza PJ (2005) Bioelectrochemistry 66:79
37. Kulesza PJ, Skunik M, Baranowska B, Miecznikowski K, Chojak M, Karnicka K, Frackowiak E, Béguin F, Kuhn A, Delville MH, Starobrzynska B, Ernst A (2006) Electrochim Acta 51:2373
38. Skunik M, Baranowska B, Fattakhova D, Miecznikowski K, Chojak M, Kuhn A, Kulesza PJ (2006) J Solid State Electrochem 10:168
39. Lisowska-Oleksiak A, Nowak AP, Jasulaitiene V (2006) Electrochem Commun 8:107
40. Ocypa M, Michalska A, Maksymiuk K (2006) Electrochim Acta 51:2298
41. Koncki R, Wolfbeis OS (1998) Anal Chem 70:2544
42. Derwinska K, Miecznikowski K, Koncki R, Kulesza PJ, Glab S, Malik MA (2003) Electroanalysis 15:1843
43. Kulesza PJ, Miecznikowski K, Chojak M, Malik MA, Zamponi S, Marassi R (2001) Electrochim Acta 46:4371
44. Kulesza PJ, Miecznikowski K, Malik MA, Galkowski M, Chojak M, Caban K, Wieckowski A (2001) Electrochim Acta 46:4065
45. Kulesza PJ, Chojak M, Karnicka K, Miecznikowski K, Palys B, Lewera A, Wieckowski A (2004) Chem Mater 16:4128
46. Kulesza PJ, Chojak M, Miecznikowski K, Lewera A, Malik M, Kuhn A (2002) Electrochem Commun 4:510
47. Bard AJ, Faulkner LR (2001) Electrochemical methods: fundamentals and applications, 2nd edn. Wiley, New York
48. Kulesza PJ, Malik MA, Wieckowski A (eds) (1999) Interfacial electrochemistry, ch 37 “Solid-state voltammetry”. Marcel Dekker, New York
49. Ilieva M, Tsakova V (2004) Synth Met 141:287